NAKAJIMA, Y., MORIMOTO, N. & WATANABE, E. (1975). *Proc. Jpn Acad.* **51**, 173-178.
NAKAJIMA, Y. & RIBBE, P. H. (1981). *Am. Mineral.* **66**, 142-147.
O'KEEFE, M. A. & BUSECK, P. R. (1979). *Trans. Am. Crystallogr. Assoc.* **15**, 27-46.
SAALFELD, H. (1979). *Neues Jahrb. Mineral. Monatsh.* **3**, 305-316.
SAALFELD, H. & GUSE, W. (1981). *Neues Jahrb. Mineral. Monatsh.* **4**, 145-150.
SADANAGA, R., TOKONAMI, M. & TAKEUCHI, Y. (1962). *Acta Cryst.* **15**, 65-68.
SAXTON, W. O., PITT, T. J. & HORNER, M. (1979). *Ultramicroscopy*, **4**, 343-354.
SCHRYVERS, D., SRIKRISHNA, K., O'KEEFE, M. A. & THOMAS, G. (1988). *J. Mater. Res.* **3**, 1355-1361.
SMITH, D. G. W. & MCCONNELL, J. D. C. (1966). *Mineral. Mag.* **35**, 810-814.
SMITH, D. J., SAXTON, W. O., O'KEEFE, M. A., WOOD, G. J. & STOBBS, W. M. (1983). *Ultramicroscopy*, **11**, 263-282.
SPENCE, J. C. H. (1980). *Experimental High Resolution Electron Microscopy*. Oxford: Clarendon Press.
TOKONAMI, M., NAKAJIMA, Y. & MORIMOTO, N. (1980). *Acta Cryst.* A**36**, 270-276.
TORRECILLAS, R. (1987). Unpublished work; thesis in progress.
YLA-JAASKI, J. & NISSEN, H. U. (1983). *Phys. Chem. Miner.* **10**, 47-54.

Acta Cryst. (1990). A**46**, 962-969

Vertex Frequencies in Generalized Penrose Patterns

BY E. ZOBETZ AND A. PREISINGER

Institut für Mineralogie, Kristallographie und Strukturchemie, Technische Universität Wien, Getreidemarkt 9, A-1060 Vienna, Austria

(*Received* 14 *March* 1990; *accepted* 16 *July* 1990)

Abstract

The grid method has been used to calculate the frequencies of the different vertices and corresponding Voronoi polygons occurring in generalized Penrose patterns. A simplified purely geometrical description of the importance of the $\sum \gamma_j = 0 \pmod 1$ relation for Penrose patterns that obey certain necessary matching conditions is given. In n-grids with n odd, local $2n$-fold symmetry occurs only if the inequality $n \cos\alpha/(1+\cos\alpha) \pmod 1 < \sum \gamma_j < n/(1+\cos\alpha) \pmod 1$, where $\alpha = \pi/n$, is fulfilled. n-grids and their corresponding rhombus patterns show global $2n$-fold symmetry if $\sum \gamma_j = 1/2 \pmod 1$, where $\gamma_j = 1/2 \pmod 1$.

Introduction

The theoretical importance of non-periodic tilings arose first from their relevance to questions of mathematical logic. Berger (1966) was the first to discover an aperiodic set consisting of 20 426 Wang tiles (only translations allowed) and therefore refuted Wang's (1961, 1975) conjecture that no aperiodic sets exist. Berger himself (Grünbaum & Shepard, 1987), Knuth (1968) and Läuchli (Grünbaum & Shepard, 1987) were able to reduce considerably the number of necessary tiles. Through a new idea of R. Ammann (Robinson, 1978), 16 is now the least-known number of Wang tiles in an aperiodic set. In 1971, Robinson discovered a set of six tiles (rotations and reflections allowed), which are basically squares with modifications to their corners and sides. Ammann (Grünbaum & Shepard, 1987) described another set of six tiles, which are of similar nature.

Some years ago, Penrose (1974, 1978, 1979) found a pair of rhombi which, when matched according to certain rules (coloured arrows or edge modifications), is forced to tile the plane in a non-periodic way. In both rhombi all sides have length a. The thick rhombus has angles of 72 and 108 ° and the thin rhombus 36 and 144 °. They have areas $A_{\text{thick}} = a^2 \sin(2\pi/5)$ and $A_{\text{thin}} = a^2 \sin(\pi/5) = A_{\text{thick}}/\tau$, where $\tau = (5^{1/2}+1)/2$ ($\simeq 1{\cdot}6180$). In any Penrose pattern the fraction of thick rhombi equals $\tau/(1+\tau)$ and the fraction of thin rhombi equals $1/(1+\tau)$. Therefore, the area covered by thick rhombi is τ^2 times greater than the area covered by thin rhombi.

Two approaches to the analysis and generation of Penrose tilings, the grid method and the projection formalism have been suggested by de Bruijn (1981). These two methods were generalized and extended by Beenker (1982), Kramer (1982), Mackay (1982), Kramer & Neri (1984), Duneau & Katz (1985), Conway & Knowles (1986), Gähler & Rhyner (1986), Levine & Steinhardt (1986), Jannsen (1986), Korepin, Gähler & Rhyner (1988) and Whittaker & Whittaker (1988). Considerable progress in the knowledge of non-periodic tilings has been made during the last few years. For an excellent review the reader is referred to Grünbaum & Shepard (1987).

In the present article, special attention is given to the Penrose tilings and their construction by means of de Bruijn's grid method. The main concern here will be the calculation of the frequencies of the

0108-7673/90/120962-08$03.00

different vertices and corresponding Voronoi polygons occurring in generalized Penrose patterns.

Pentagrids: de Bruijn's algebraic theory of Penrose tilings

Since we have followed de Bruijn's grid method, it seems appropriate to recall his approach to the analysis of Penrose tilings.

An infinite Penrose tiling consists of strips of adjacent rhombi with parallel edges. Through connecting the midpoints of the parallel edges we get curves that stay inside the strips. de Bruijn shows that these curves can be distorted without topological changes into five periodic line-grids (the union of which is called a pentagrid) perpendicular to the pentagonal directions $e_j = \{\cos(2j\pi/5), \sin(2j\pi/5)\}$, with $j = 0, 1, 2, 3, 4$. Every pentagrid tiling is dual to a Penrose tiling by Penrose rhombi, and conversely. A pentagrid is called regular if no three lines are concurrent, else it is called singular. An intersection point* in the pentagrid corresponds to a rhombus, a mesh, which is the open region between grid lines, corresponds to a vertex of the rhombus pattern, and an edge of a mesh corresponds to an edge of a rhombus.

Using de Bruijn's complex notation the jth grid is the set

$$\{z \in C \,|\, \mathrm{Re}\,(z\zeta^{-j}) + \gamma_j \in Z\},$$

where z is the coordinate of a point in the complex plane C, $\zeta = \exp(2\pi i/5)$, and Z is the set of integers. $\mathrm{Re}\,(z\zeta^{-j})$ denotes the real part of $z\zeta^{-j}$. The γ_j are real numbers which in Penrose patterns, the case studied by de Bruijn, satisfy the relation $\sum \gamma_j = 0 \pmod 1$. We associate with every point z five integers

$$K_j(z) = \lceil \mathrm{Re}\,(z\zeta^{-j}) + \gamma_j \rceil,$$

where $\lceil a \rceil$ is the smallest integer greater than a. As the $K_j(z)$ change only when we cross a line of the corresponding grid, they are constant for a given mesh. The quantity $K = \sum K_j(z)$ is called the index of a vertex (every mesh of the pentagrid corresponds to a vertex of the rhombus pattern). The index increases by 1 when we move a point along an edge of a rhombus in the directions $\zeta^0, \zeta^1, \zeta^2, \zeta^3, \zeta^4$, and decreases by 1 when we move it in the directions $-\zeta^0, -\zeta^1, -\zeta^2, -\zeta^3, -\zeta^4$.

In order to determine the bounds of $\sum K_j(z)$ we introduce five real numbers λ_j defined as follows:

$$\lambda_j(z) = K_j(z) - \mathrm{Re}\,(z\zeta^{-j}) - \gamma_j.$$

Summation over j yields

$$\sum K_j(z) = \sum \lambda_j(z) + \sum \gamma_j,$$

since $\sum \mathrm{Re}\,(z\zeta^{-j}) = 0$. Since $0 \le \lambda_j(z) < 1$ and the left-hand side is an integer, we can distinguish between two cases:

$$(a)\ \sum \gamma_j = \text{integer} \Rightarrow \sum K_j(z) \in \{\textstyle\sum \gamma_j + 1, \sum \gamma_j + 2, \sum \gamma_j + 3, \sum \gamma_j + 4\},$$

$$(b)\ \sum \gamma_j \neq \text{integer} \Rightarrow \sum K_j(z) \in \{\lceil \textstyle\sum \gamma_j \rceil, \lceil \sum \gamma_j \rceil + 1, \lceil \sum \gamma_j \rceil + 2, \lceil \sum \gamma_j \rceil + 3, \lceil \sum \gamma_j \rceil + 4\}.$$

Importance and geometrical interpretation of the relation $\sum \gamma_j = 0 \pmod 1$

One of the relevant features of Penrose tilings that are compatible with the matching conditions enforcing non-periodicity is that there are no vertex configurations with three adjacent thin rhombi (Fig. 1*b*). It can easily be deduced that a corresponding line configuration in the dual pentagrid (Fig. 1*a*) appears only if

$$d_{23}/d_{14} > 1 + \tau,$$

where d_{23} is the distance between two consecutive intersection points on a line of the 0th grid with lines of the 2nd and 3rd grid, respectively. Analogously, d_{14} is the distance between two consecutive intersection points on a line of the 0th grid with lines of the 1st and 4th grid, respectively. From geometrical considerations (Appendix 1*) it follows that

$$d_{23}/d_{14} = \tau\{(c + \textstyle\sum \gamma_j) \pmod 1\}/c \pmod 1,$$

where

$$c = \gamma_0/\tau - \gamma_1 - \gamma_4 + k_0/\tau.$$

* Table 2, Appendix 1 and Appendix 2 have been deposited with the British Library Document Supply Centre as Supplementary Publication No. SUP 53375 (7pp.). Copies may be obtained through The Technical Editor, International Union of Crystallography, 5 Abbey Square, Chester CH1 2HU, England.

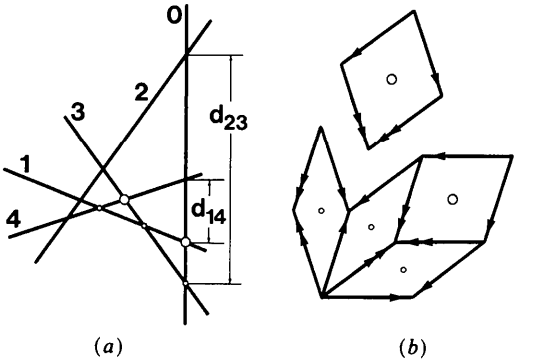

Fig. 1. Grid-line configuration (*a*) that is not compatible with matching conditions (*b*) (single and double arrows) which force a non-periodic tiling of the plane.

* Since we exclude singular pentagrids, the grid lines partition the plane into polygons to form a tiling with 4-valent vertices.

The following two cases may be distinguished:

(*a*) $\sum \gamma_j = \text{integer} \Rightarrow d_{23}/d_{14} = \tau$

(*b*) $\sum \gamma_j \neq \text{integer} \Rightarrow$

$$0 \leq d_{23}/d_{14} \leq \tau[\textstyle\sum \gamma_j \pmod 1]$$

$$\text{if } (c + \textstyle\sum \gamma_j) \pmod 1 / c \pmod 1 > 1$$

$$\text{and } \tau/\{1 - [\textstyle\sum \gamma_j \pmod 1]\} \leq d_{23}/d_{14} \leq \infty$$

$$\text{if } (c + \textstyle\sum \gamma_j) \pmod 1 / c \pmod 1 \leq 1.$$

Therefore, the ratio d_{23}/d_{14} for every line of the 0th grid is less than $1+\tau$ if and only if $\sum \gamma_j = 0 \pmod 1$. The corresponding values for all the other grids may be obtained by cyclic permutation.

n-grids (*n* odd) with local or global 2*n*-fold symmetry

One of the characteristic features of n grids with n odd is that, once the lines with $k_j = 0$ are chosen, the quantity $\sum \gamma_j$ is unaffected by the choice of the origin from which the shifts γ_j are measured (Socolar & Steinhardt, 1986). Translation of the origin to a point v changes each γ_j as follows:

$$\Delta\gamma_j = \text{Re}\,(v\zeta^{-j}).$$

Since $\sum \text{Re}\,(v\zeta^{-j}) = 0$ it follows that $\sum \Delta\gamma_j = 0$.

In n-grids with n even, which are obtained by superposition of n ordinary grids, obtained from each other by rotation over angles of multiples of π/n, the quantity $\sum \gamma_j$ is unaffected by shifting the origin along a line that is normal to the vector

$$\mathbf{e} = \{\cos[(n-1)\pi/2n], \sin[(n-1)\pi/2n]\}$$

and goes through the origin.

Owing to this property of n-grids with n odd and since we are not interested in the specific values of k_j, we may shift the origin inside a certain mesh such that all the γ's become greater than 0 and less than 1.

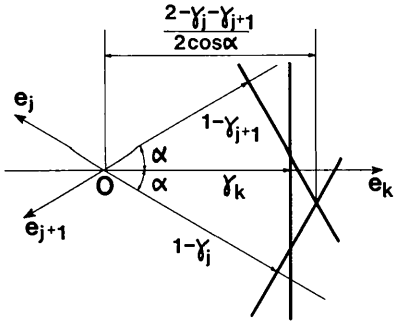

Fig. 2. Part of a grid-line configuration that corresponds to local or global 2*n*-fold symmetry with n odd. The direction e_k bisects the two consecutive grid directions e_j and e_{j+1}, where $k = (j + \lceil n/2 \rceil) \pmod n$. As can be seen, the line of the kth grid only participates in the mesh surrounding the origin O if $\gamma_k < (2 - \gamma_j - \gamma_{j+1})/2 \cos\alpha$, where $\alpha = \pi/n$.

Table 1. *Lower* (b_l) *and upper* (b_u) *bounds of* $\sum \gamma_j$ *for n-grids* (*n odd*) *with local* 2*n-fold symmetry with* $5 \leq n \leq 25$

$b_l = n\cos(\pi/n)/[1+\cos(\pi/n)] \pmod 1$.
$b_u = n/[1+\cos(\pi/n)] \pmod 1 = 1 - b_l$.
Global 2*n*-fold symmetry occurs if $\sum \gamma_j = 1/2 \pmod 1$, where each γ_j takes the value $1/2 \pmod 1$.

n	b_l		b_u	
5	0·2361	$(\sim 2\tau - 3)$	0·7639	$(\sim 4 - 2\tau)$
7	0·3177		0·6823	
9	0·3601		0·6399	
11	0·3863		0·6137	
13	0·4042		0·5958	
15	0·4171		0·5829	
17	0·4270		0·5730	
19	0·4348		0·5652	
21	0·4410		0·5590	
23	0·4462		0·5538	
25	0·4505		0·5495	

From Fig. 2 it can be deduced that the two grid lines with index $k = (j + \lceil n/2 \rceil) \pmod n$ participate in the mesh surrounding the origin only if the following two inequalities hold:

$$\gamma_k < (1 - \gamma_j + 1 - \gamma_{j+1})/2\cos\alpha$$

and

$$1 - \gamma_k < (\gamma_j + \gamma_{j+1})/2\cos\alpha,$$

where $\alpha = \pi/n$. Since we are interested in the dependence on $\sum \gamma_j$ of n-grids with local or global 2n-fold symmetry, we have to sum over j to obtain the necessary condition that all the $2n$ relevant grid lines participate in the mesh under investigation to form either a regular (global 2n-fold symmetry) or an irregular (local 2n-fold symmetry) 2n-gon and obtain

$$n - \textstyle\sum \gamma_j < 2\sum \gamma_j/2\cos\alpha$$

and

$$\textstyle\sum \gamma_j < (2n - 2\sum \gamma_j)/2\cos\alpha.$$

The two inequalities can be summarized to give

$$n\cos\alpha/(1+\cos\alpha) < \textstyle\sum \gamma_j < n/(1+\cos\alpha).$$

The bounds can be reduced modulo 1 without loss of generality. Table 1 gives the bounds of $\sum \gamma_j$ for n-grids with $5 \leq n \leq 25$. Global 2n-fold symmetry occurs if $\sum \gamma_j = 1/2 \pmod 1$, where each γ_j takes the value $1/2 \pmod 1$.

Vertex frequencies in generalized Penrose patterns

de Bruijn (1981) introduced the set

$$V = \{(\textstyle\sum \lambda_j, \sum \lambda_j \zeta^{2j}) \,|\, 0 < \lambda_j < 1\},$$

which has the property that any type of vertex is made visible by means of a corresponding point in the set V. By assuming $\sum \gamma_j = 0$ the points of V with $\sum \gamma_j = s$ form the pentagon-shaped regions V_s. Since $\sum \lambda_j = \sum K_j(z)$ and $K_j(z) \in \{1, 2, 3, 4\}$, we have the four

regions V_1, V_2, V_3 and V_4, which correspond to cross sections of four equidistant planes with a rhombic icosahedron (Henley, 1986).

By means of the set V we can answer the question whether a vector $(k_0, \ldots, k_4) \in Z^5$ corresponds to a mesh in a given pentagrid such that $K_0(z) = k_0, \ldots, K_4(z) = k_4$. Such a mesh exists if and only if

$$\{\sum k_j, \sum (k_j - \gamma_j)\zeta^{2j}\} \in V. \qquad (1)$$

Moreover, we can see which of the adjacent points obtained by increasing or decreasing just one k_j by 1 or by adding $\pm\zeta^{2j}$ satisfy (1).*

Consider vertices with $\sum k_j = 2$. The points $\theta = \sum (k_j - \gamma_j)\zeta^{2j}$ densely fill the pentagon-shaped region V_2 ($\sum \gamma_j = 0$) depicted in Fig. 3(*a*). Adjacent vertices are derived in the following way. If a point θ lies inside the shaded area, the addition of $+\zeta^2$ (k_1+1), $+\zeta^8$ (k_4+1) and -1 (k_0-1) will yield points that lie inside the corresponding subsets V_3 and V_1, respectively. We can, however, derive the type of vertex simply by forming the intersections of V_2 with the accordingly shifted subsets V_1 and V_3. Fig. 3(*b*) shows the division of the pentagonal region V_2 ($\sum \gamma_j = 0$) into polygonal subregions according to the different types of vertices.

In fact, the type of a vertex in a Penrose pattern is entirely defined by the location of θ in V_s, where $s = \sum k_j$. Since the points θ that satisfy (1) densely fill the regions V_s, the frequency of each vertex type can be derived by means of the areas of the corresponding subregions.

In the case where $\sum \gamma_j$ = integer there are now five subsets V_s, since

$$\sum k_j \in \{\lceil \sum \gamma_j \rceil, \lceil \sum \gamma_j \rceil + 1, \lceil \sum \gamma_j \rceil + 2, \lceil \sum \gamma_j \rceil + 3, \lceil \sum \gamma_j \rceil + 4\}.$$

Three of them, $V_{\lceil \sum \gamma_j \rceil + 1}$, $V_{\lceil \sum \gamma_j \rceil + 2}$, and $V_{\lceil \sum \gamma_j \rceil + 3}$ are decagonal shaped, $V_{\lceil \sum \gamma_j \rceil}$ and $V_{\lceil \sum \gamma_j \rceil + 4}$ are pentagons. Their division into polygonal subregions depending on $\sum \gamma_j$ is shown in Fig. 4. Since we have made no use of any matching condition such as coloured arrows for the calculation of the vertex frequencies, we obtain only 16 types of vertices (Fig. 5) in generalized Penrose patterns. The frequencies of the different vertices are evaluated by calculating the areas of the corresponding regions of the subsets V_s. The results are summarized in Tables 2* and 3 and Figs. 6 and 7.

Extension of de Bruijn's colouring theorem (Pavlovitch & Kléman, 1987) yields 41 types of vertices.† Pavlovitch & Kléman use four different rhombi and distinguish between two types of grid lines: the lines of type 1 at the left of which the index has the values $\lceil \sum \gamma_j \rceil$, $\lceil \sum \gamma_j \rceil + 1$ and $\lceil \sum \gamma_j \rceil + 2$, and lines of type 2 where the index takes the values $\lceil \sum \gamma_j \rceil + 1$, $\lceil \sum \gamma_j \rceil + 2$ and $\lceil \sum \gamma_j \rceil + 3$.‡

Another way we can classify the vertices is to construct the Voronoi domains. The Voronoi domain of a particular point from a set of discrete points in two-dimensional space is the innermost region bounded by lines that perpendicularly bisect the lines from the point under consideration to all other points. In consequence, the Voronoi domain is the polygon enclosing the space in which all points are closer to that point than to any other. Voronoi polygons may be used to define neighbour bonds. Any point whose Voronoi polygon shares an edge with the polygon of the central point is counted as a neighbour. The number of neighbours is the coordination number of the central point. In fact there are only three kinds of neighbour bonds in Penrose tilings (Fig. 5): those at distance *a*, which corresponds to a rhombus edge,

* Note that ± 1, $\pm\zeta$, $\pm\zeta^2$, $\pm\zeta^3$, $\pm\zeta^4$ on p. 51 in de Bruijn (1981) should be replaced by ± 1, $\pm\zeta^2$, $\pm\zeta^4$, $\pm\zeta^6$, $\pm\zeta^8$.

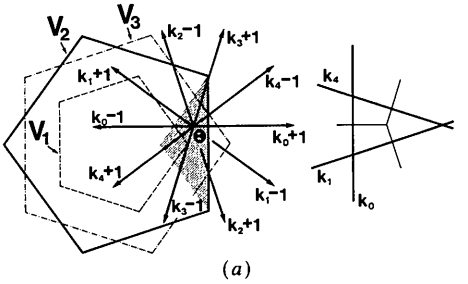

(*a*)

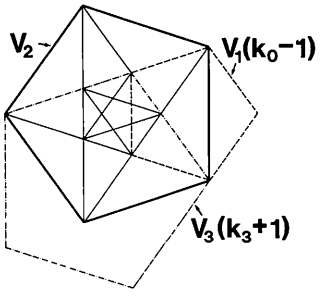

(*b*)

Fig. 3. (*a*) Subset V_2 of a pentagrid with $\sum \gamma_j = 0 \pmod 1$ and a point $\theta = \sum (k_j - \gamma_j)\zeta^{2j}$ that satisfies (1). The ten vectors $k_j \pm 1$ correspond to points we obtain by increasing or decreasing only one k_j by 1 or by addition of $\pm\zeta^{2j}$. Three of them, $k_1 + 1$ $(+\zeta^2)$, $k_4 + 1$ $(+\zeta^8)$, and $k_0 - 1$ (-1) lie inside the corresponding subsets V_3 and V_1. The type of vertex is shown on the right-hand side of V_2. We get the same type of vertex if θ lies inside the shaded area. (*b*) Division of the subset V_2 into polygonal subregions according to different types of vertices. The subregions are derived by intersection of V_2 with accordingly shifted subsets V_1 and V_3. One of each subset is shown, namely V_1, corresponding to $k_0 - 1$, and V_3, which corresponds to $k_3 + 1$.

* See deposition footnote.

† Note that ${}^8W$, ${}^8_1W$, ${}^8_3W$ and ${}^7V$, ${}^7_1V$ in Fig. 11 on p. 699 in Pavlovitch & Kléman (1986) should be replaced by ${}^7V$, ${}^7_1V$, ${}^7_3V$ and ${}^7W$, ${}^7_1W$, respectively.

‡ Note that their equation (13) on p. 695 which determines the type of a line is not correct. In Appendix 2 (deposited) is given the derivation of an equation which determines the type of a grid line according to the extended colouring theorem.

bonds along short diagonals of thin rhombi at distance $c = a/\tau$ and along short diagonals of thick rhombi at distance $b = 2a \sin(\pi/5)$. If we denote by na, nb and nc the number of a, b and c bonds we get the numbers shown in Table 3. Following Euler's relationship between the numbers of elements of different dimensionality in a structure, we get the equation $e/m - e/n + 1 = 0$, where e is the average number of edges of the tiles, and m and n denote the average domain valencies of vertices and edges,

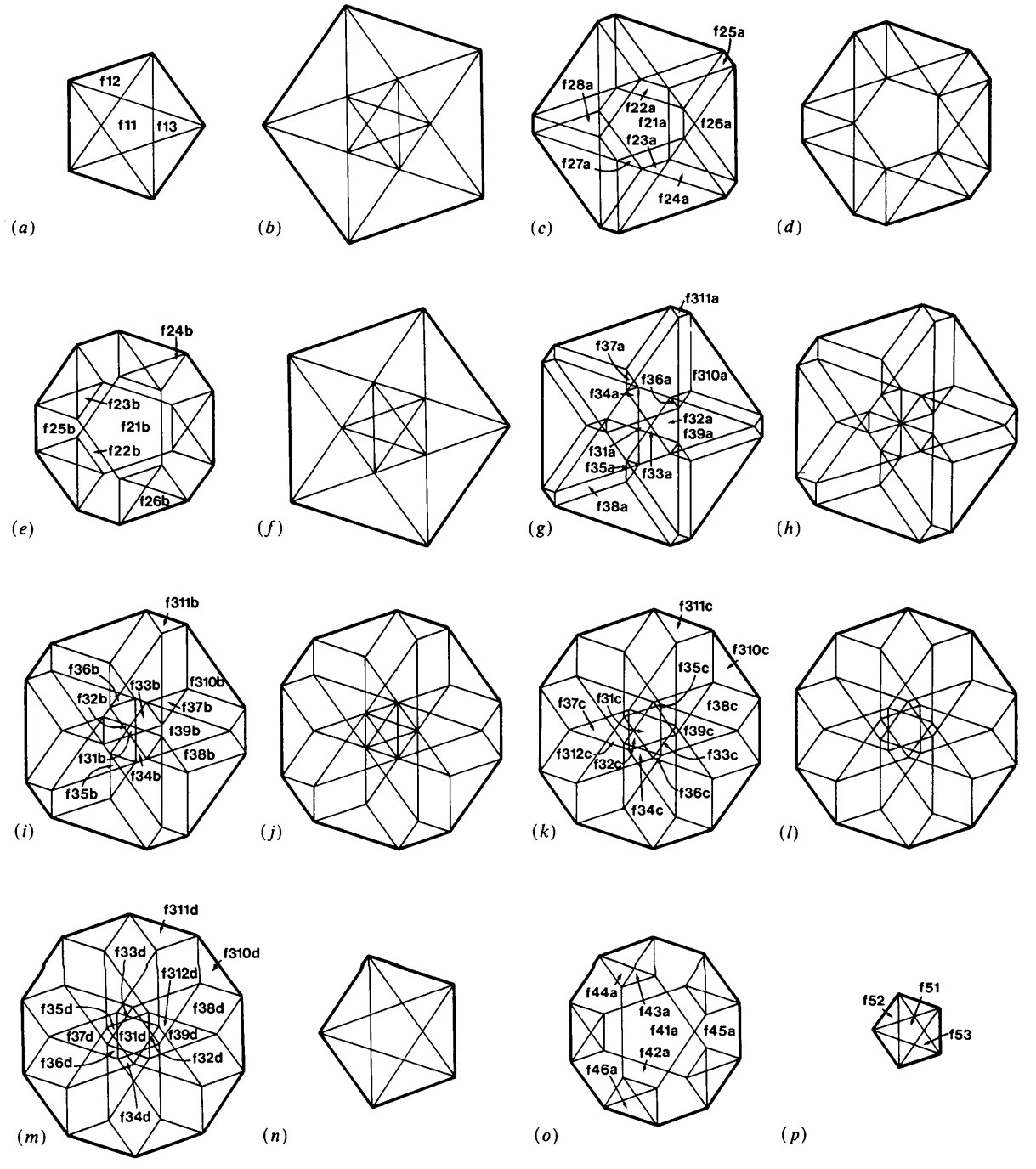

Fig. 4. Division of the five subsets V_s ($s = \sum k_j$) into polygonal subregions depending on $\sum \gamma_j$. (*a*) $s = 1$, $\sum \gamma_j = 0$. (*b*) $s = 2$, $\sum \gamma_j = 0$. (*c*) $s = 2$, $\sum \gamma_j = 0{\cdot}2$. (*d*) $s = 2$, $\sum \gamma_j = 2 - \tau$ ($\sim 0{\cdot}3820$). (*e*) $s = 2$, $\sum \gamma_j = 0{\cdot}5$. (*f*) $s = 3$, $\sum \gamma_j = 0$. (*g*) $s = 3$, $\sum \gamma_j = 0{\cdot}15$. (*h*) $s = 3$, $\sum \gamma_j = 2\tau - 3$ ($\sim 0{\cdot}2361$). (*i*) $s = 3$, $\sum \gamma_j = 0{\cdot}3$. (*j*) $s = 3$, $\sum \gamma_j = 2 - \tau$ ($\sim 0{\cdot}3820$). (*k*) $s = 3$, $\sum \gamma_j = 0{\cdot}44$. (*l*) $s = 3$, $\sum \gamma_j = 4\tau - 6$ ($\sim 0{\cdot}4721$). (*m*) $s = 3$, $\sum \gamma_j = 0{\cdot}5$. (*n*) $s = 4$, $\sum \gamma_j = 0$. (*o*) $s = 4$, $\sum \gamma_j = 0{\cdot}4$. (*p*) $s = 5$, $\sum \gamma_j = 0{\cdot}5$.

respectively. In Penrose tilings $e=4$ and $n=2$, so $m=4$, which corresponds to the average number na of a bonds meeting at a vertex. Each vertex in the Voronoi tiling is common to three polygons, so the equation $e/m-e/n+1=0$ is satisfied only if e takes the value 6, since $n=2$. From this it follows that the average coordination number $na+nb+nc=6$, and since $na=4$ and the number of thick rhombi is τ times greater than the number of thin rhombi, we obtain $nb=2/\tau$ and $nc=2/\tau^2$.

The frequencies of larger local environments, corresponding to first- and higher-coordination spheres, may be obtained by the intersection of a particular polygonal subregion with accordingly shifted subsets V_s. For instance, in Penrose tilings with $\sum \gamma_j=0$, each S vertex with index 1 or 4 is surrounded by five

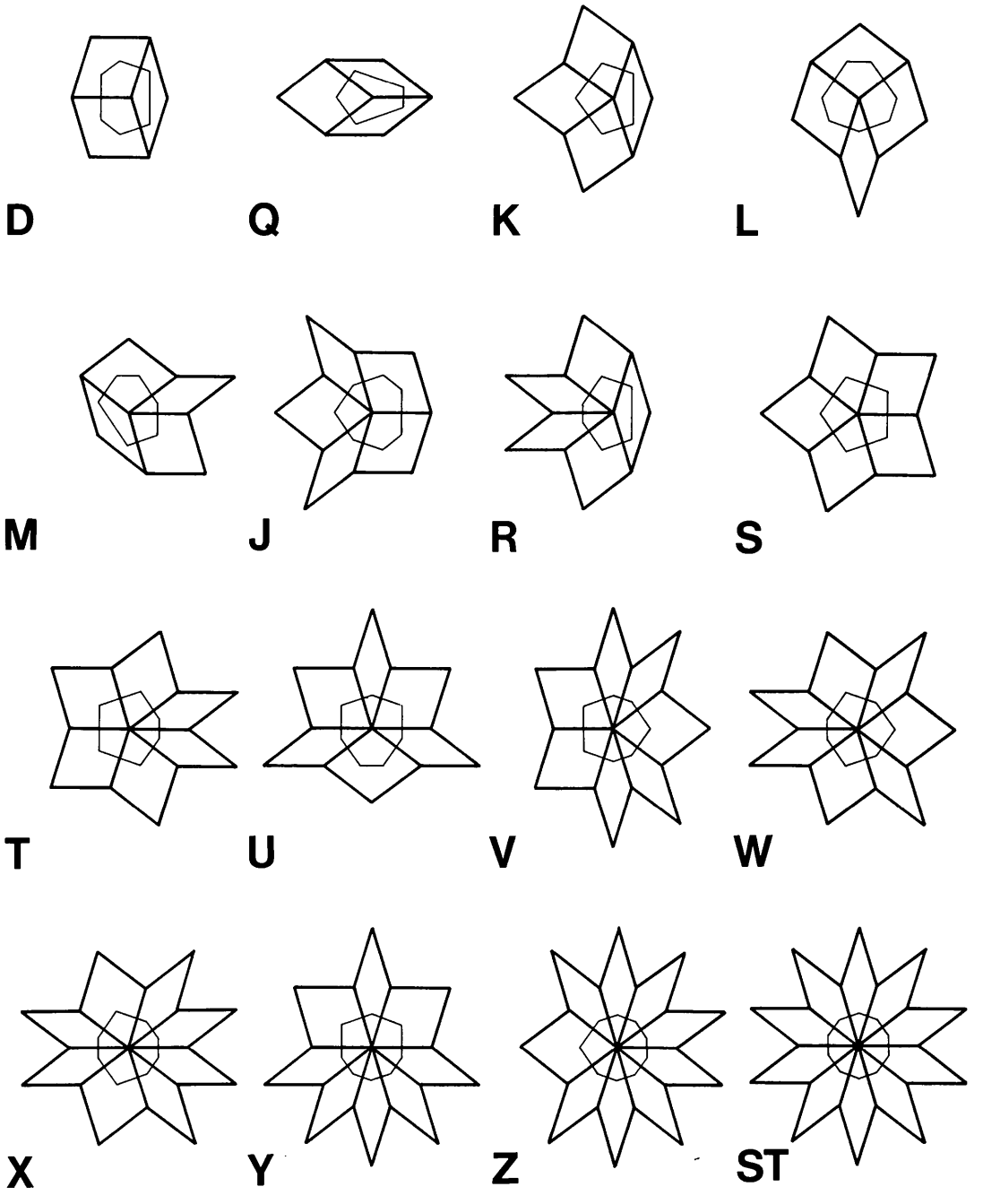

Fig. 5. The 16 types of vertices (thick lines) and corresponding Voronoi domains (thin lines) occurring in generalized Penrose patterns. The notation is in accordance with de Bruijn (1981) and Pavlovitch & Kléman (1987).

Table 3. *Frequencies F of the different vertices in generalized Penrose patterns*

The first column gives the notation of the vertices v according to de Bruijn (1981) and Pavlovitch & Kléman (1987). The second column contains the number of edges ev meeting at a vertex. The next four columns contain the frequencies F given by the sum of the corresponding areas f of the subsets V_s depending on $\sum \gamma_j$ ($0 \le \sum \gamma_j \le 0{\cdot}5$). The areas ad (in arbitrary units) of the Voronoi domains and their number of edges ed are given in columns 7 and 8, respectively. The last three columns contain the numbers of a, b and c bonds. Since Penrose patterns are metrically balanced (Grünbaum & Shepard, 1987), the relations $\sum ev_v F_v / \sum F_v = 4$ and $\sum ed_v F_v / \sum F_v = 6$ ($\sum F_v = 4+2\tau$) must be satisfied.

		F								
v	ev	$0 \le \sum \gamma_j \le 2\tau-3$	$2\tau-3 \le \sum \gamma_j \le 2-\tau$	$2-\tau \le \sum \gamma_j \le 4\tau-6$	$4\tau-6 \le \sum \gamma_j \le 1/2$	ad	ed	na	nb	nc
D	3	$f26a+f310a+f311a+f46a$	$f26a+f310b+f311b+f46a$	$f26b+f310c+f311c+f46a$	$f26b+f310d+f311d+f46a$	$3\tau+5$	6	3	2	1
Q	3	$f12+f25a+f45a+f52$	$f12+f25a+f45a+f52$	$f12+f25b+f45a+f52$	$f12+f25b+f45a+f52$	$4\tau+1$	5	3	0	2
K	4	$f13+f42a+f53$	$f13+f42a+f53$	$f13+f22b+f42a+f53$	$f13+f22b+f42a+f53$	$7\tau-2$	5	4	0	1
L	4	$f38a$	$f38b$	$f38c$	$f38d$	$3\tau+7$	7	4	3	0
M	4	$f24a+f44a$	$f24a+f44a$	$f24b+f44a$	$f24b+f44a$	$4\tau+3$	6	4	1	1
J	5	$f28a+f37a+f39a$	$f28a+f37b+f39b$	$f37c+f39c$	$f37d+f39d$	$4\tau+5$	7	5	2	0
R	5	$f23a+f43a$	$f23a+f43a$	$f23b+f43a$	$f23b+f43a$	$5\tau+1$	6	5	0	1
S	5	$f11+f21a+f31a+f41a+f51$	$f11+f21a+f41a+f51$	$f11+f21b+f41a+f51$		$10\tau-5$	5	5	0	0
T	6	$f22a+f33a$	$f22a$			$8\tau-2$	6	6	0	0
U	6	$f35a$	$f35b$	$f312c$	$f312d$	$5\tau+3$	7	6	1	0
V	7	$f27a+f32a$	$f27a+f32b$			$6\tau+1$	7	7	0	0
W	7	$f36a$	$f36b$	$f34c+f36c$	$f34d+f36d$	$6\tau+1$	7	7	0	0
X	8	$f34a$	$f34b$	$f33c$		$4\tau+4$	8	8	0	0
Y	8			$f35c$	$f35d$	$4\tau+4$	8	8	0	0
Z	9		$f33b$	$f32c$	$f32d+f33d$	$2\tau+7$	9	9	0	0
ST	10		$f31b$	$f31c$	$f31d$	10	10	10	0	0

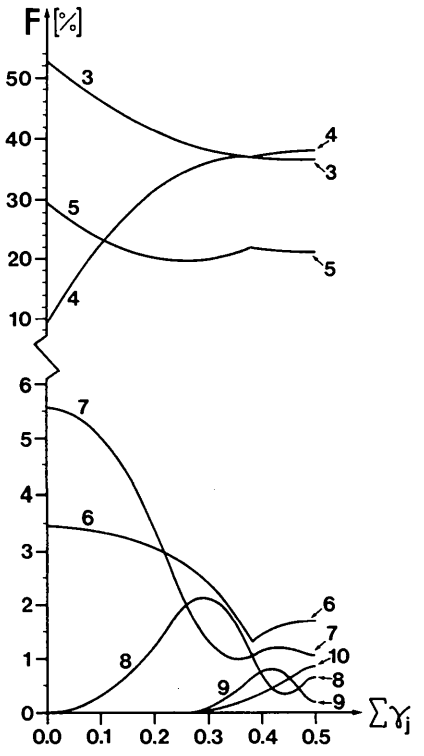

Fig. 6. Frequency of n-valent vertices ($n = 3, \ldots, 10$) *versus* $\sum \gamma_j$ ($0 \le \sum \gamma_j \le 0{\cdot}5$) in generalized Penrose patterns.

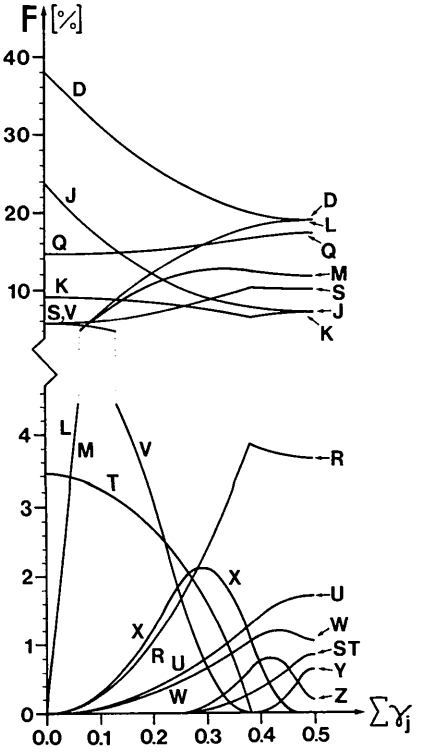

Fig. 7. Frequency of the 16 types of vertices *versus* $\sum \gamma_j$ ($0 \le \sum \gamma_j \le 0{\cdot}5$) in generalized Penrose patterns.

Table 4. *Neighbour separations r and their frequencies in Penrose tilings with* $\sum \gamma_j = 0$

The neighbour points are described by $\sum \Delta k_j \zeta^j$. Cyclic permutations and changes of signs give points with equivalent distances.

r		Δk_j	Frequency	
$\tau-1$	(0·6180)	10100	$4-2\tau$	(0·7639)
1		10000	4	
$(3-\tau)^{1/2}$	(1·1756)	$1\bar{1}000$	$8-4\tau$	(1·5279)
$(4-\tau)^{1/2}$	(1·5434)	$1\bar{1}010$	$8\tau-12$	(0·9443)
τ	(1·6180)	11000	$16\tau-23$	(2·8885)
τ	(1·6180)	11001	$33-20\tau$	(0·6393)
$(\tau+2)^{1/2}$	(1·9021)	$10\bar{1}00$	$9-3\tau$	(4·1459)
2		20000	$10-6\tau$	(0·2918)
$(\tau+3)^{1/2}$	(2·1490)	$11\bar{1}00$	$7\tau-7$	(4·3262)
$2\tau-1$	(2·2362)	$11\bar{1}0\bar{1}$	$4-2\tau$	(0·7639)
$(2\tau+3)^{1/2}$	(2·4972)	$111\bar{1}0$	$16-8\tau$	(3·0557)
$\tau+1$	(2·6180)	$110\bar{1}0$	$6\tau-4$	(5·7082)

D-vertices. The second coordination sphere consists of either five *J*-, four *J*- and one *V*- or three *J*- and two *V*-vertices, with relative frequencies $2\tau-1$, 5 and 5τ, respectively. The first coordination sphere of a *Q*-vertex consists of two *J*- and one *V*-, or two *J*- and one *T*-vertex. The first-mentioned coordination is 2τ times more frequent than the second one. The environment of a *V*-vertex up to the second coordination sphere always looks the same. The environments of *T*-vertices differ only if the fourth coordination sphere is taken into account.

The derivation of the frequencies of larger local environments was used to calculate the radial distribution function among all vertices in Penrose tilings with $\sum \gamma_j = 0$. The neighbour separations up to a maximum distance of $r = \tau^2 a$ are listed in Table 4.

By means of deflation, Henley (1986) derived the frequencies of the different vertices in Penrose patterns with $\sum \gamma_j =$ integer. Whittaker & Whittaker (1988) extended the self-similarity relationships to more general cases. They derived 14 decomposition types for Penrose patterns with $\sum \gamma_j = 1/2 \pmod 1$, where $\gamma_j = \sum \gamma_j/5$. However, when the γ's depart from simple values by arbitrarily small amounts, the number of decomposition types becomes indefinitely large. Hence Henley's method seems not to be appropriate to determine the vertex frequencies in generalized Penrose patterns.

References

BEENKER, F. P. M. (1982). Report 82-WSK-04. Eindhoven Univ. of Technology, Eindhoven, The Netherlands.

BERGER, R. (1966). *Mem. Am. Math. Soc.* No. 66.

BRUIJN, N. G. DE (1981). *Proc. K. Ned. Acad. Wet. Ser. A*, **43**, 39-52, 53-66.

CONWAY, J. H. & KNOWLES, K. M. (1986). *J. Phys. A*, **19**, 3645-3653.

DUNEAU, M. & KATZ, A. (1985). *Phys. Rev. Lett.* **54**, 2688-2691.

GÄHLER, F. & RHYNER, J. (1986). *J. Phys. A*, **19**, 267-277.

GRÜNBAUM, B. & SHEPARD, G. C. (1987). *Tilings and Patterns.* New York: W. H. Freeman.

HENLEY, C. L. (1986). *Phys. Rev. B*, **34**, 797-816.

JANNSEN, T. (1986). *Acta Cryst.* A**42**, 261-271.

KNUTH, D. E. (1968). *The Art of Computer Programming*, Vol. 1. Reading, MA: Addison-Wesley.

KOREPIN, V. E., GÄHLER, F. & RHYNER, J. (1988). *Acta Cryst.* A**44**, 667-672.

KRAMER, P. (1982). *Acta Cryst.* A**38**, 257-264.

KRAMER, P. & NERI, R. (1984). *Acta Cryst.* A**40**, 580-587.

LEVINE, D. & STEINHARDT, P. J. (1986). *Phys. Rev. B*, **34**, 596-616.

MACKAY, A. L. (1982). *Physica (Utrecht)*, **114**A, 609-613.

PAVLOVITCH, A. & KLÉMAN, M. (1987). *J. Phys. A*, **20**, 687-702.

PENROSE, R. (1974). *Bull. Inst. Math. Appl.* **10**, 266-271.

PENROSE, R. (1978). *Eureka*, **39**, 16-22.

PENROSE, R. (1979). *Math. Intell.* **2**, 32-37.

ROBINSON, R. M. (1971). *Invent. Math.* **12**, 177-209.

ROBINSON, R. M. (1978). *Invent. Math.* **44**, 259-264.

SOCOLAR, J. E. S. & STEINHARDT, P. J. (1986). *Phys. Rev. B*, **34**, 617-647.

WANG, H. (1961). *Bell Syst. Tech. J.* **40**, 1-41.

WANG, H. (1975). *Fundam. Math.* **82**, 295-305.

WHITTAKER, E. J. W. & WHITTAKER, R. M. (1988). *Acta Cryst.* A**44**, 105-112.

Acta Cryst. (1990). A46, 970-974

Computer Simulation of Size Effect from Orientationally Disordered Molecular Crystals: Monoclinic Dibromodiethyldimethylbenzene

BY RITA KHANNA

Materials Science Division, Indira Gandhi Centre for Atomic Research, Kalpakkam 603 102, *India*

AND T. R. WELBERRY

Research School of Chemistry, Australian National University, PO Box 4, *Canberra, ACT* 2601, *Australia*

(*Received* 24 *May* 1990; *accepted* 17 *July* 1990)

Abstract

Size-effect distortions have been computed in a pair of orientationally disordered isomers of dibromodiethyldimethylbenzene using Monte Carlo simulation. Net forces/torques were computed for each molecule and the direction of movement was determined using variational methods. The sampling was carried out both in sequential and in a random manner. Effects of lattice size, interaction radius and boundary conditions have been investigated. In the lowest-energy configuration, typical centre-of-mass displacements were in the range 0·25–0·30 Å. Average molecular librations, represented in terms of Eulerian angles, were in the range 0–4°. The φ and ψ components however had large r.m.s. values (~10°). Basic results and trends were unaffected by the lattice size and the interaction radius (6–15 Å). However, the r.m.s. values of the angles came down considerably for fixed boundaries. The influence of temperature on size effect has also been investigated.

1. Introduction

In recent publications (Welberry, Jones & Epstein, 1982; Epstein & Welberry, 1983; Welberry & Siripitayananon, 1986, 1987) we have described our interest in the study of disordered molecular crystals, and the development of methods for recording and analysing diffuse X-ray scattering data. Although the most recent of these studies involved quantitative fitting of calculated three-dimensional-disorder diffuse-scattering distributions to the observed data, no account was taken of thermal diffuse scattering nor the molecular equivalent of the size-effect distortions that are found to be important in alloys (Warren, Averbach & Roberts, 1951). In a more recent paper (Khanna & Welberry, 1987) general diffraction equations for diffuse scattering from molecular crystals, taking account of these additional effects, were developed, and a basic analysis scheme for separating the various components of the diffuse scattering was outlined. This work showed that the analysis for molecular crystals is considerably more complex than the analogous analysis for alloys because of several factors: the slowly varying and essentially spherical atomic scattering factors f_A *etc.* applicable to the alloy case must be replaced by molecular scattering factors, which are rapidly varying complex functions in the reciprocal space; alloys also tend to be relatively simple structures with high symmetry whereas molecular crystals are generally of low (*e.g.* monoclinic) symmetry; perhaps most importantly, molecular crystals often contain different sublattices upon which the molecules have a different (symmetry-related) orientation.

Before embarking on an analysis of the diffuse scattering from a real sample, we decided, in order to obtain some feeling for the relative magnitudes of the various effects likely to be encountered in practice, to undertake a computational study using semi-empirical potential-energy calculations (see *e.g.* Kitaigorodsky, 1973; Ramdas & Thomas, 1978) on the previously reported dibromodiethyldimethylbenzene system [BEMB1 and BEMB2 (Fig. 1); see Welberry & Siripitayananon (1986, 1987)]. Both BEMB1 and BEMB2 are monoclinic with two molecules per unit cell. Their lattice parameters are:

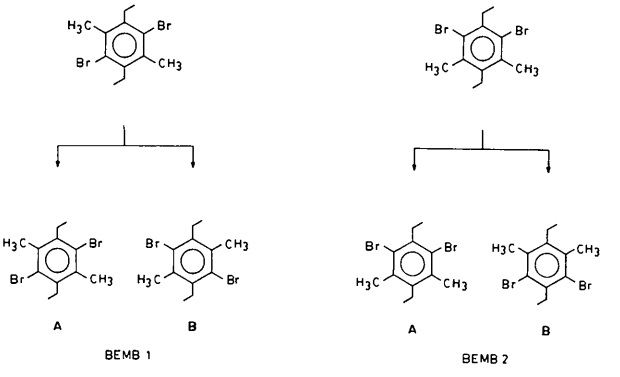

Fig. 1. Molecular structures of two isomers BEMB1 and BEMB2 which possess static orientational disorder. Two possible orientations, *A* and *B*, are shown in the figure.

0108-7673/90/120970-05$03.00